JOURNAL OF OPTOELECTRONICS AND ADVANCED MATERIALS Vol. 12, No. 9, September 2010, p. 1869 - 1878

Magnetic properties of iron-palladium solid solutions and compounds

E. BURZO*, P. VLAIC[a]
Faculty of Physics, Babes-Bolyai University RO-400084 Cluj-Napoca, Romania
[a]*University of Medicine and Pharmacy "Iuliu Hatieganu", Physics and Biophysics Department Cluj-Napoca, Romania*

Band structure calculations were performed on disordered Fe_xPd_{100-x} solid solutions as well as on FePd and $FePd_3$ ordered compounds. The equilibrium values of the lattice parameters, magnetic moments, Curie temperatures, pressure effects as well as spontaneous volume magnetostrictions were obtained and compared with the experimental data. A good description of experimental results has been shown. The magnetic properties were correlated with distances between iron atoms, as suggested by the Néel-Slater curve.

(Received August 24, 2010; accepted September 15, 2010)

Keywords: Fe-Pd alloys, Magnetic properties, Spontaneous magnetostriction

1. Introduction

The Fe-Pd alloys system has a complex phase diagram [1]-Fig.1. At high temperatures, below solidus line, the presence of γ-Fe_xPd_{100-x} solid solutions, having fcc type structure, is shown in all the composition range. At room temperature, the α-Fe_xPd_{100-x}, alloys, having the bcc type structure, have been reported for $x \geq 70$ and fcc-type lattice for $x \leq 60$ [2,3]. In the composition range $70 \leq x \leq 75$ four phases with different tetragonal distortions, following a Bain transformation path from fcc to bcc-type lattice have been reported [4,5].

When decreasing temperature the alloys having compositions around x=50 and 25 at % Fe exhibit a typical disorder-order process. The disordered fcc-type structure, with $40 \leq x \leq 50$, having low magnetic anisotropy, orders to $L1_0$ type superstructure via a thermodynamically first order type, order-disorder transformation. The ordered structure is tetragonal via an alternating stacking of Fe and Pd planes along the [001] principal axis with respect to fcc-lattice. The axial ratio c/a is smaller than the unity ($c/a \cong 0.96$), due to the difference of atomic radii between Fe and Pd. In the composition range $40 \leq x \leq 50$, a disordered fcc phase was obtained by homogenezing the alloys, at 1200 °C, and then quenching [6]. The ordered $L1_0$ phase was obtained by annealing the above alloys at 500 °C. The other ordered phase is $FePd_3$, which crystallizes in $L1_2$-type structure having $Pm\bar{3}m$ space group. This phase can exist at room temperature, in the composition range $14 \leq x \leq 38$ [1].

The disordered Fe_xPd_{100-x} alloys with $60 \leq x \leq 70$ are known for their Invar property [7,8]. The alloy with x=68.8 showed a giant magnetostriction of ≅ 3 %, at 77 K [9]. In the composition range $60 \leq x \leq 70$, the spontaneous volume magnetostriction scales linearly on the square of magnetization [10]. The magnetic shape memory effect has been shown around $Fe_{70}Pd_{30}$ disordered fct phase [11].

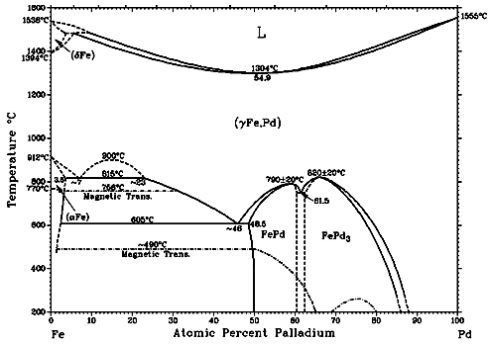

Fig. 1. Phase diagram of Fe-Pd alloys [1].

The magnetic properties of Fe_xPd_{100-x} alloys were studied [6,10,12-21]. The Curie temperatures of the atomic ordered alloys having $40 \leq x \leq 50$ at % Fe decrease by ≅30 K, as compared to those of disordered phase [6]. The saturation magnetization diminishes, from 3.3 μ_B in $Fe_{60}Pd_{40}$ to 3.0 μ_B in $Fe_{50}Pd_{50}$. In the composition range $20 \leq x \leq 70$, the resultant magnetizations decrease linearly with increasing Pd content [10]. The Curie temperatures have a maximum at x=50. The presence of a magnetic moment of 0.35 μ_B has been reported on Pd atom [16]. An increase of the iron moment with Pd content up to 18 at % has been also shown. For this composition, a value of 3.0 μ_B/Fe atom has been reported.

The Fe_xPd_{100-x} alloys with $x \geq 76.8$ [16] or $x \geq 80$ [22], were studied by Mössbauer effect at ^{57}Fe nucleus. A distribution function of the hyperfine fields, B_{hf}, has been shown. According to Delyagin et al [22], the distribution has a discrete structure, defined by variations of the contributions to B_{hf} from magnetic moments of neighbouring iron atoms. An instability of configurations with a large total spin and the formation of local spin configurations with an antiferromagnetic orientation of

magnetic moments has been also reported.

Magnetic scattering of neutrons was measured in Fe_xPd_{100-x} alloys with $10 \leq x \leq 15$ [23]. Satellite diffuse peaks at $1 \pm \delta,0,0$ were found. The wave vector of spin modulation varied with iron concentration. The experimental data suggested that the oscillatory spin component homogeneously coexist with the ferromagnetic long-range order.

A combination of bulk magnetization, conversion electron Mössbauer spectroscopy and polarized neutron reflectometry studies, showed that in Pd/Fe multilayers, at 4.5 K, there is a slight ($\cong$ 10 %) enhancement of the Fe moment at the Pd/Fe interface and that the Pd is almost maximally polarized with an average moment of 0.32 μ_B to a depth of $\cong$ 20 Å, from the Pd/Fe interface [24].

Band structure calculations were performed on some Fe-Pd alloys, particularly on those atomic ordered, having equiatomic composition [25-41]. Galanakis et al [24] used both local spin density approximation (LSDA) and generalized gradient approximation (GGA) methods to study the electronic structure of fct-$Fe_{50}Pd_{50}$ compound. The same compound was investigated by using LSDA, with first principle full-potential muffin-tin orbital calculations including orbital correction [26]. A full potential linear augmented plane wave (FLAPW) method was also used [27]. Yamada et al [28,29] analysed the electronic structure of FePd compound by a linear muffin-tin orbital method (LMTO) within atomic sphere approximation (ASA), where a generalized gradient corrections for exchange-correlation potential was taken into account The calculated magnetic moments of 3.04 μ_B/Fe atom and 0.32 μ_B/Pd atom describe well the observed magnetization per formula unit [42]. The electronic structures of FePd, $FePd_3$ and of hypothetical compound Fe_3Pd were investigated by employing the augmented spherical wave (ASW) method [30]. The total energy was computed as function of volume and magnetic moment by performing fixed spin moment calculations. The FePd compound showed the usual behaviour of a strong itinerant ferromagnet. The iron states, formed rather localized bands in $FePd_3$. The stability of the ordered alloys was investigated as function of the iron content. The hypothetical $L1_2$ structure of Fe_3Pd was shown to be at least metastable with respect to corresponding disordered alloys [43]. The ordered magnetic moments in FePd were also computed by Mohri et al [31], Mazzoni [32], Gonzalez et al [33], Sakuma et al [34] and Barabash et al [35]. The coherent potential approximation (CPA) method has been used to study the electronic structure of fct-$Fe_{70}Pd_{30}$ alloy [36]. The magnetocrystalline anisotropy of $Fe_{70}Pd_{30}$ [37] has been determined in the local spin density approximation with Perdew-Wang [38] parameterization of exchange and correlation potential. The electronic structure of hypothetical compound Fe_3Pd, close to the above composition, has been also discussed [39].

There are only few studies of the electronic structure of Fe_xPd_{100-x} solid solutions. The Korrringa-Kohn-Rostoker Green's function method with the local-density functional approximation was used to obtain the magnetic moment at the Pd site and to predict that dilute substitutions of Pd in bcc Fe will cause an increase in the magnetization of the bulk alloy [41]. The electronic structures and magnetic properties of Fe_xPd_{100-x} alloys with $50 \leq x \leq 85$ were investigated in the framework of density functional theory, using the full potential approximation [40]. The origin of the tetragonal distortion in the Fe-Pd magnetic shape memory alloys was found to be a Jahn-Teller effect.

Previously [44], we reported the band structure calculations performed on Fe_xPt_{100-x} alloys, as well as on FePt and Fe_3Pd ordered phases. A good agreement between the computed values of the lattice parameters, magnetic moments, Curie temperatures, as well as spontaneous volume magnetostrictions and experimental data, respectively has been shown. The spin glass behaviour, observed in fcc Fe_xPt_{100-x} alloys, when decreasing lattice parameters, simulating the pressure effects, was also discussed.

As an on going work, we report in this paper the band structure calculations performed on disordered Fe_xPd_{100-x} alloys as well as on FePd and $FePd_3$ ordered phases. As can be seen also in this case, the experimental data are rather well described by computed values.

2. Computational method

The ground state electronic structures, total energies, magnetic properties, spontaneous volume magnetostrictions of α- and γ-Fe_xPd_{100-x} disordered alloys, as well as of FePd and $FePd_3$ ordered compounds, have been studied by means of spin polarized and scalar relativistic tight-binding linear muffin tin orbital method (TB-LMTO) within atomic sphere approximation (ASA), together with the coherent potential approximation (CPA), in order to describe the random Fe-Pd alloys [45,46]. The LSDA was used for the exchange correlation potential of the electron gas, assuming the Vosko-Wilk-Nussair parameterization [47]. The initial electronic configurations were taken as core $+3d^64s^2$ for Fe and core $+4d^{10}5s^0$ for Pd. The structures of α- and γ-phases were assumed to be bcc and fcc, respectively. The Wigner-Seitz radii of Fe and Pd constituents are determined in agreement with ASA requirement and have been considered to be equal for disordered phases and different for ordered compounds. A spd-basis set has been used for both atoms. All band structure calculations have been performed by using a mesh of 24x24x24 k-points in the full Brillouin zone (BZ) resulting in 413 k-points in the irreducible wedge of BZ, that ensure the accuracy of the total energy better than 10^{-2} mRy. The magnetic disorder has been analysed within disorder local moment (DLM) formalism [48], by treating the binary alloys as pseudoternary $Fe^{\uparrow}_{x-c}Fe^{\downarrow}_{c}Pd_{100-x}$ ones, with (x-c) atoms having spin-up state and c-atoms being in the state with spin-down. The DLM configuration with c=0 will describe the ferromagnetic (FM) ground state, while that with c=x/2 has been considered as a paramagnetic (PM) state, which shows no resultant magnetic moment. Really, this state is antiferromagnetic, in which the antiparallel alignment of magnetic moments are compensated, miming the PM state. We note that the PM DLM states are fundamentally different from non-magnetic (NM) states (where M=0), considered in the present calculations.

3. Results

3.1 Disordered Fe_xPd_{100-x} alloys

3.1.1. Lattice parameters

Total energy calculations have been performed on γ-Fe_xPd_{100-x} with $0 < x \leq 80$ and α-Fe_xPd_{100-x} with $75 \leq x \leq 100$ alloys in both FM and NM states. The total energies, ΔE_t, as a function of lattice parameters, for samples with x = 25, 50, 75, 85, 90 and 95 are plotted in Fig.2. For fcc solid solutions, at lower values of the lattice constants, the total energies are degenerate. When the lattice constants are higher, the FM state is the stable one. In case of α-Fe_xPd_{100-x} solid solutions only stable solutions with finite magnetizations are shown.

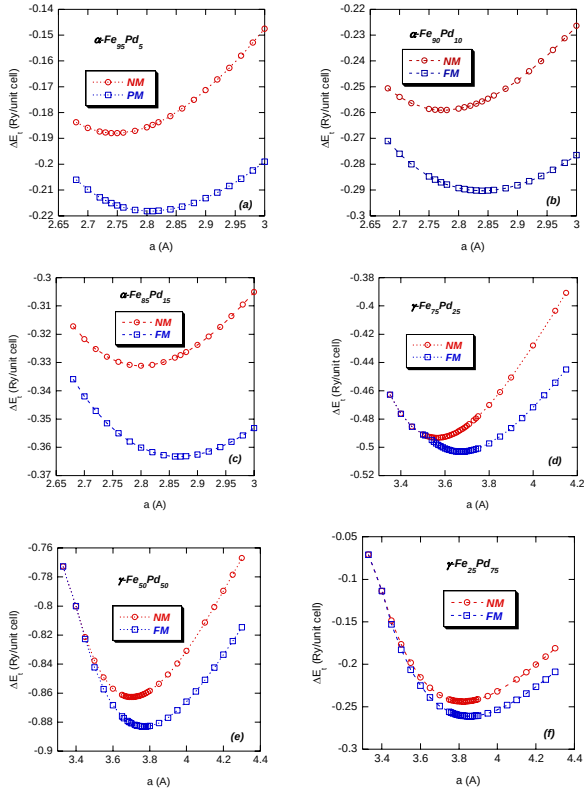

Fig. 2. Total energies as function of lattice spacings for α-$Fe_{95}Pd_5$ (a), α-$Fe_{90}Pd_{10}$ (b), α-$Fe_{85}Pd_{15}$(c) γ-$Fe_{75}Pd_{25}$ (d), γ-$Fe_{50}Pd_{50}$ (e) and γ-$Fe_{25}Pd_{75}$ (f) solid solutions.

The equilibrium values of the lattice parameters have been determined from a third-order polynominal interpolation of the total energy. The replacement of Fe atoms by Pd ones result in an increase of the equilibrium lattice spacings. The computed values are in rather good agreement with experimental data [10,20,49], as shown in Fig.3a, for γ-Fe_xPd_{100-x} solid solutions. The agreement is not so good in case of α-Fe_xPd_{100-x} solid solutions-Fig.3b. Although show the same composition dependence as experimental values, these are smaller by 0.05-0.06Å. The difference between the two sets of data may be attributed to the LSDA approximation used in the present calculations and the well known underestimation of the equilibrium lattice constants in case of bulk iron alloys.

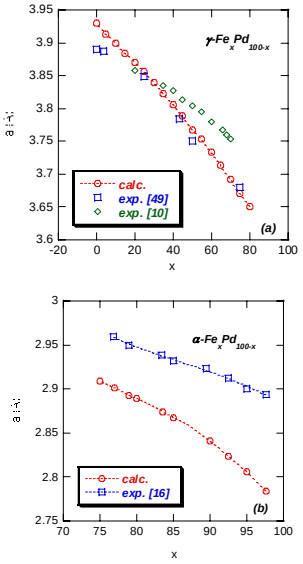

Fig.3 Composition dependences of computed lattice parameters for (a) γ-Fe_xPd_{100-x} alloys with $0 < x \leq 75$. The experimental data [10,49] are also given. In (b) are plotted the computed lattice parameters of α-Fe_xPd_{100-x} with $x > 74$. The experimental data [16] are also included.

The matter of differences between the experimental and calculated lattice constants has been already discussed [50]. Correct results, from band structure calculations, based on experimental lattice parameters, can be also obtained. As example, in YCo_2 compound, realistic electronic structure calculations with a fully self consistent procedure has been considered in order to solve the corresponding multi-orbital Hubbard Hamiltonian. A many-body solver was used which is a modified version of the fluctuating exchange approximation which takes into account fluctuations in the particle-particle and particle-hole channel for the multi-orbital case.

3.1.2 Magnetic moments

The atom resolved spin polarized density of states (DOS) for Fe and Pd in γ-Fe_xPd_{100-x} with x=25, 50, 75 and α-Fe_xPd_{100-x} with x=85, 90 and 95 solid solutions are shown in Fig. 4. Smooth DOS are shown, due to chemical disorder that smeared the electronic states. The iron atoms, in γ-Fe_xPd_{100-x} alloys, exhibit a strong ferromagnetism with almost completely filled majority spin sub-bands. A small contribution to DOS from a majority spin sub-band can be shown for iron in α-Fe_xPd_{100-x} (x=85,90,95). Thus, the energy of states, at the Fermi level, are generally mostly of minority spin character. The composition dependences of the Fe and Pd magnetic moments, at the equilibrium lattice

constants, as well as the average magnetizations per formula unit, are shown in Fig.5.

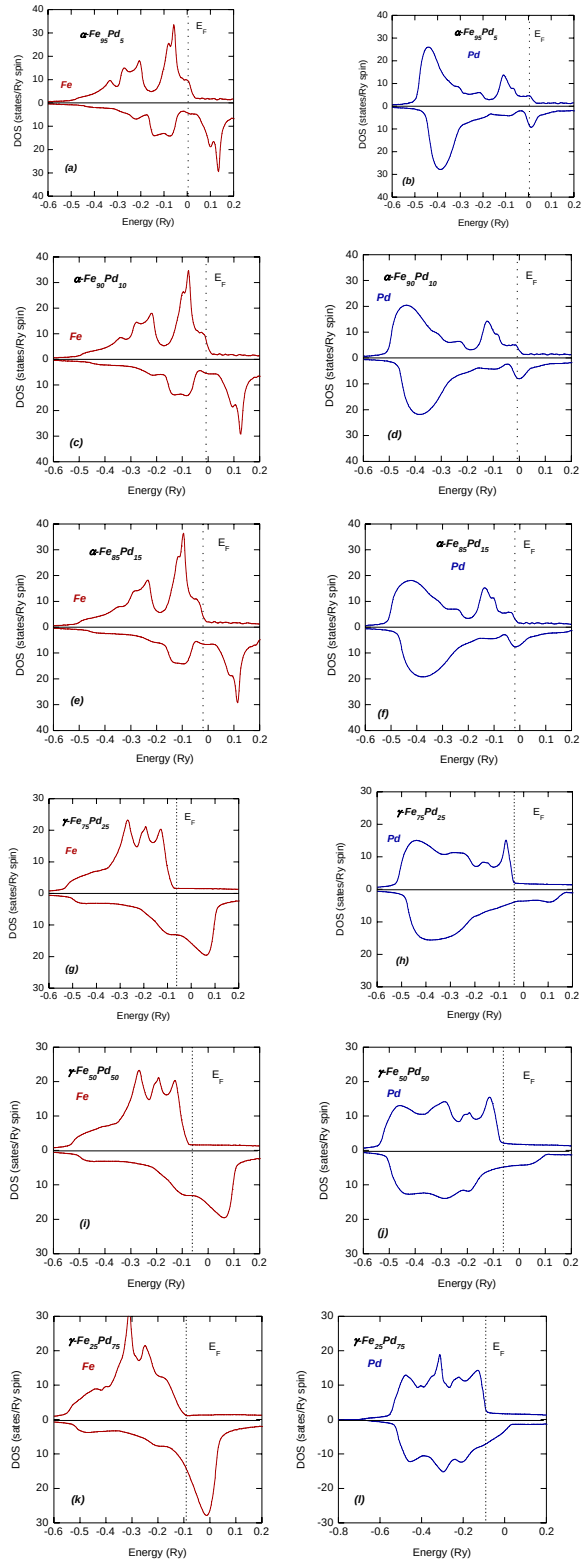

Fig.4. Densities of states for Fe and Pd, in α-Fe_xPd_{100-x} with x=95, 90, 85, and γ-Fe_xPd_{100-x} with x=75, 50, 25 solid solutions.

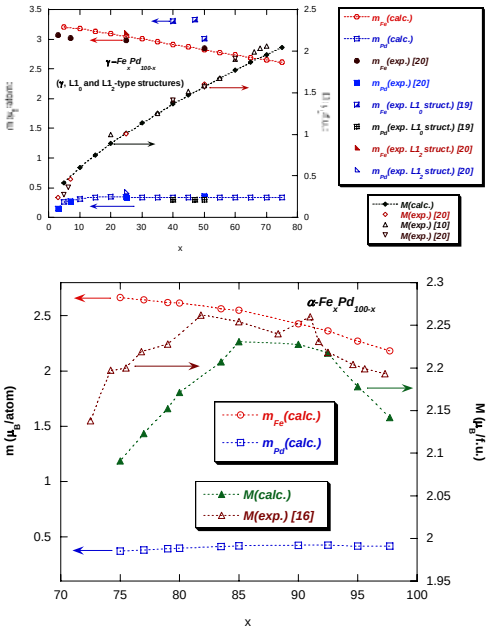

Fig.5. Composition dependences of the iron an palladium moments in γ- and α-Fe_xPd_{100-x} solid solutions and the magnetic moments per formula unit. The experimental data [3,10,16,19,20] are also plotted.

A polarization of Pd4d band, paralelly oriented to iron moments, is shown. This behaviour can be correlated with the presence of short range Fe3d-Pd4d exchange interactions. As result of the hybridization of Pd4d band with Fe3d one, the Pd4d band is split. Their splitting can be correlated with the intensity of exchange interactions, the number of Fe atoms situated in the neighbouring of a Pd site, respectively. As a result, the Pd4d band polarizations increase in γ-Fe_xPd_{100-x} up to x=15, above this composition being saturated-Fig.5. The Pd4d band-polarization experimentally determined [13,14], of 0.35μ_B/atom or 0.40μ_B/atom in Pd/Fe multilayers [51], agree well with the computed values. In α-Fe_xPd_{100-x} solid solutions there is also an increase of Pd band polarization for $75 \leq x \leq 85$, and then the Pd moments saturate at somewhat higher values than in γ- Fe_xPd_{100-x} alloys-Fig.5.

The iron magnetic moments of γ-Fe_xPd_{100-x} alloys, increase when the Pd content is higher – Fig.5. This can be correlated with an increase of the minority spin state density at the Fermi level, attributed to Fe3d band hybridization effects. The computed magnetic moments in the $40 \leq x \leq 50$ range are in rather good agreement with the values determined by neutron diffraction studies, at room temperature, and then extrapolated to T= 0 K [19].

Since the iron moments are nearly one order of magnitude higher than the palladium contributions to magnetization, the magnetic moments per formula unit will increase, as function of iron content. The calculated values are nearly the same as experimentally ones [3,10], for γ-Fe_xPd_{100-x}, in the composition range $x \leq 60$. Slight deviations can be seen in the range of $60 \leq x \leq 80$ at % Fe.

In case of α-Fe_xPd_{100-x} solid solutions, the calculated values show a maximum at x=92 decreasing both when iron content increases or decreases from the above value. Similar behaviour was shown experimentally [2,16].

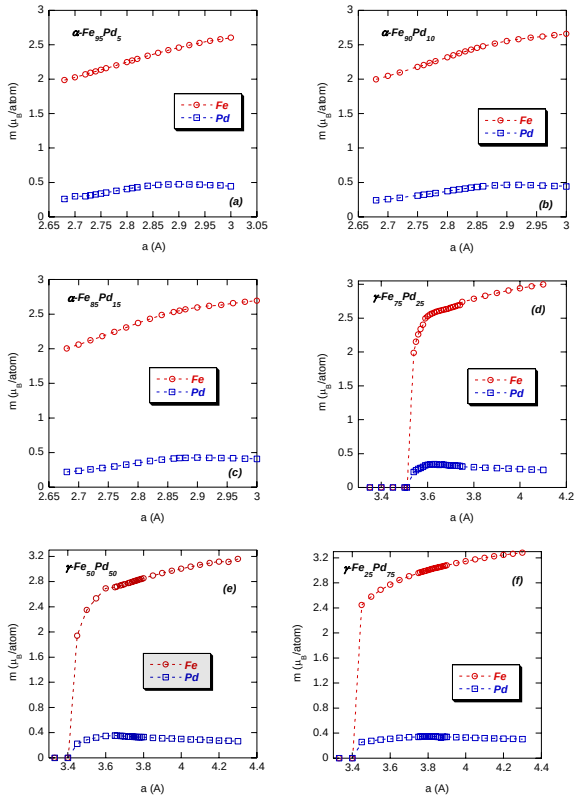

Fig. 6. Dependences of Fe and Pd magnetic moments on the lattice parameters for α-Fe_xPd_{100-x} with x=95,90,85 (a-c)and γ-Fe_xPd_{100-x} with x=75,50,25 (d-f) solid solutions.

The dependences of iron moments and Pd4d band polarizations on the lattice parameters, simulating the pressure effects, were studied – Fig.6. In case of γ-Fe_xPd_{100-x} solid solutions, at smaller lattice constants, the total energies of ferromagnetic and NM states are degenerate and there are stable solutions for M=0. As a result, a NM state, can be stable at high pressures. This corresponds to a critical value of the lattice parameters a_c, which decrease when increasing Pd content, a_c= 3.50 Å (x=75), 3.42 Å (x=50) and 3.40 Å (x=25). These involves reductions of lattice parameters, from their equilibrium values, at 0.955 (x=75), 0.91 (x=50) and 88.2 (x=25). This behaviour can be correlated with the distances between iron atoms, d_{Fe}. According to Néel [52], the exchange interactions, J_{Fe}, between iron atoms are dependent on their separation. Neglecting the contributions of Pd atoms to the exchange interactions, the J_{Fe} values will decrease both by increasing and decreasing distances between iron atoms, from a characteristic value s=d_{Fe}-2r, where r is the iron ionic radius (r=0.72Å). The s value corresponding to maximum of exchange interactions, after Néel, was located at s ≅ 1.32 Å. In addition, the exchange interactions are negative for a critical value d_{Fe} which corresponds to s=1.06 Å-Fig.7. The s values describing the transition from magnetic to non-magnetic states are 1.036 Å (x=75), 0.978 Å (x=50) and 0.964 Å (x=25). All the above values suggest the presence of antiferromagnetic interactions at these s values. In case of γ-Fe_xPd_{100-x} solid solutions, and supposing the random distribution of constituting elements in lattice, there not all the iron atoms are situated at the same interatomic distance. As Pd content is higher, the number of iron situated at larger distances, than expected, if all Fe atoms occupy lattice sites, increases. Thus, a greater diminution of lattice constants is necessary for magnetic –"non-magnetic" transition to take place as the Pd content is higher.

The effect of pressure on the Curie temperatures of γ-$Fe_{70}Pd_{30}$ [53] and $Fe_{66}Pd_{34}$, $Fe_{72}Pd_{28}$ [54] were discussed. At 7.8 GPa, a decrease of T_c value for a sample with x=70, from 610 to 400 K was shown [53]. Also at 4.2 K, the changes in magnetization with pressure were small. At RT the magnetizations decreased with pressure [54]. This can be interpreted as a decrease of Curie points with pressure and related changes of magnetization, as T/T_c values increase. As discussed already, these can be connected with a decrease of the distance between iron atoms, as predicted by Néel-Slater curve.

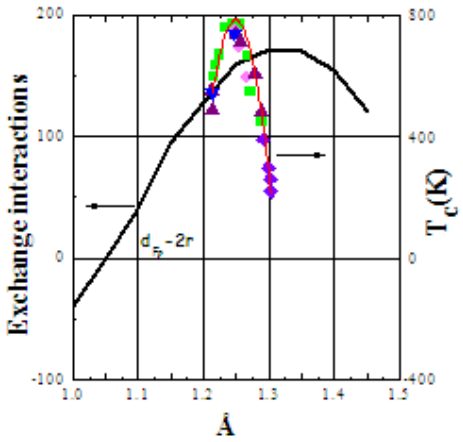

Fig. 7. The Néel-Slater curve [52] and the Curie temperatures in γ- Fe_xPd_{100-x} solid solutions, as function of s-values.

In case of α-Fe_xPd_{100-x} solid solutions, not a transition to "non-magnetic" state is suggested for a/a_c values of the order 0.8, although the expected s values are smaller than 1.06 Å. Probably, in this case, the exchange interactions with the Fe atoms situated in the second sphere of coordination are rather strong and not allowed antiferromagnetic coupling of iron moments.

The above behaviour is currently evidenced in R_2Fe_{17} and $R_2Fe_{14}B$-type compounds where R is a rare-earth or yttrium. In R_2Fe_{17} there are four types and in $R_2Fe_{14}B$ six types of iron atoms situated at different distances, some involving values s<1.06 Å [55-58]. In case of Lu_2Fe_{17}, where the distances between iron atoms are smallest, an helicoidal arrangement of the iron moments has been shown. For other R_2Fe_{17} compounds, the negative exchange

interactions are not satisfied, since the positive ones, involving the same atom with iron atoms located at larger distances, are more intense and a considerable magnetic energy is stored. The same behaviour has been shown in $R_2Fe_{14}B$ compounds. Since the negative interactions are not satisfied, the stored magnetic energy will bring on the Curie temperatures. These decrease very much, as compared to pure iron, although the number of magnetic atoms in the formula unit is 90 % from their total content. Replacement of iron involved in negative exchange interactions, even by non-magnetic atoms, will increase the Curie temperatures in both above systems [56,57].

Magnetic scattering of neutrons was measured in α-Fe_xPd_{100-x} alloys with $10 \leq x \leq 15$ [23]. In this composition range, s values situated between 1.08 and 1.099 Å, are shown. These are very close to the distance s≅1.06 Å where negative exchange interactions are supposed to be present. It is not excluded that local distortion of lattice as result of Pd substitution, to be present, some of the iron atoms being situated in sites where antiferromagnetic interactions are present. This can explain the presence of some oscillatory spin components which homogeneously coexists with ferromagnetic long range order, as experimentally observed [23].

3.1.3 Exchange interactions and Curie temperatures

The exchange interactions in γ-Fe_xPd_{100-x} solid solutions were evaluated in the mean field approximation (MFA), from the differences between energies of the ferromagnetic and "paramagnetic" DLM states. From these values we determined the Curie temperatures, T_c-Fig.8. The T_c values have maximum at a composition x=60, somewhat higher than evidenced for experimentally determined values, where the maximum is located at x=55. The difference between theoretical and experimental maxima in T_c values may be related with the single site approximation of CPA used in the present calculations and the neglecting of short-range order in these compounds compared with experimental evidence, where a certain degree of chemical short-range order is generally present even in the disordered alloys. When correlated with the distances between iron atoms, the experimentally maxima, in T_c values, are situated at s= 1.25 Å, while those computed, at 1.23 Å. On Fig.7 are also plotted the experimentally determined Curie temperatures of γ-Fe_xPd_{100-x} solid solutions. These, in the first approximation, describe the exchange interactions. in the system. There can be seen that the maximum of T_c vs s is situated at a value smaller than 1.32 Å, predicted by Néel, although the same form of dependence is shown. The shift of the maximum can be connected with the presence of Pd. The Fe3d-Pd4d exchange interactions, as well as the corresponding effects on the magnetic properties, can be a reason for a maximum localization at somewhat smaller s values that predicted by Néel [52].

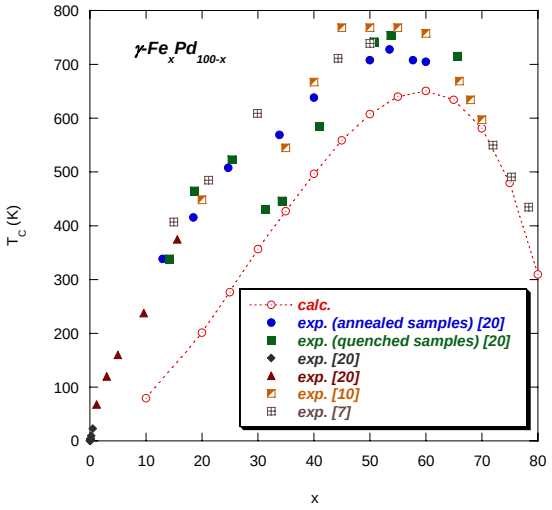

Fig. 8Curie temperatures as function of composition for γ-Fe_xPd_{100-x} solid solution. The experimental data are also plotted [7,10,20].

3.1.4 Spontaneous volume magnetostriction

The spontaneous volume magnetostriction, ω_s, is defined by the ratio between the volume difference of ferromagnetic, V(FM) and paramagnetic DLM, V(DLM), states and the volume of ferromagnetic one [59]:

$$\omega_s = \frac{V(FM) - V(DLM)}{V(FM)} \quad (1)$$

Calculated total energies as function of lattice parameters for different DLM states, in case of $Fe_{75}Pd_{25}$ and $Fe_{70}Pd_{30}$ disordered alloys are show in Fig.9. A gradual shift of the equilibrium lattice parameters to lower values is shown, when increasing the number of antiferromagnetically coupled iron pairs. This behavior is similar with that previously reported in case of Fe-Pt alloys [60] and represent the main mechanism for the presence of the Invar effect. The spontaneous volume magnetostriction can be shown in a magnetically ordered alloys for which the paramagnetic DLM minimum with a smaller lattice constant (small magnetic moment) is situated slightly above the magnetic solution with a larger lattice constant. When increasing temperature, the local minimum with a small lattice constant can be populated by thermal fluctuations which counteracts the usual thermal expansion due to lattice vibrations [61]. Néel [52] attributed the above anomaly to the magnetic energy variation as function of the volume, the distances between atoms, respectively, as a result of the magnetic coupling energies between iron spins. Also he showed that the anomaly, ω_s, at the magnetic transition temperature, is proportional to the square of the magnetization.

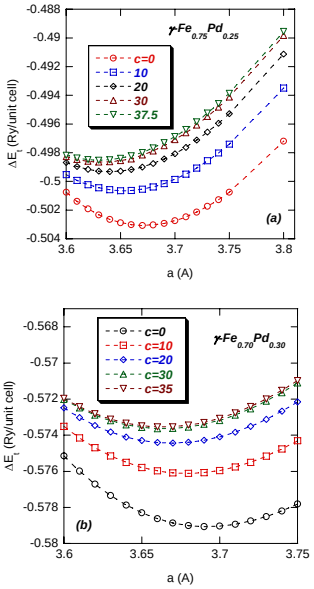

Fig.9 Total energies versus lattice constants for DLM states of γ-$Fe^{\uparrow}_{75}Fe^{\downarrow}_{25}Pd_{25}$ (a) and γ-$Fe^{\uparrow}_{70}Fe^{\downarrow}_{30}Pd_{30}$ (b) alloys.

The volume magnetostriction as function of valence electron concentration, as well as on differences between the squares of the magnetic moments, for ferromagnetic and paramagnetic DLM states, is shown in Fig.10. As previously showed [60], in case of Fe_xPt_{100-x} solid solutions, the maximum of ω_s in Fe-Pd systems corresponds to an electron concentration per atom e/a=8.5, so called magic electron number. The computed values are also close to those experimentally determined [19].

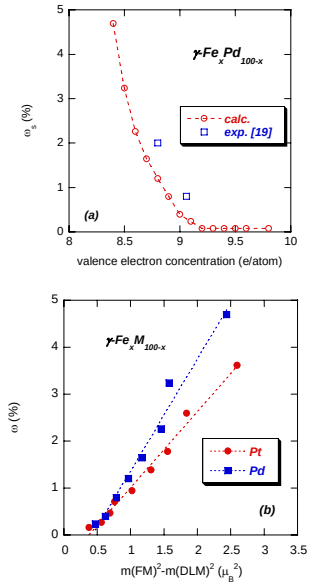

Fig. 10. Magnetostriction of γ-Fe_xPd_{100-x} solid solutions as function of valence electron concentration (a) and of difference between the squares of the moments in ferromagnetic and paramagnetic DLM states (b). Experimental data [19] are also plotted.

Néel [52] suggested that the ω_s values are linearly dependent on the difference between the square of the magnetic moments of ordered and paramagnetic states. According to Khmelevskyi et al [60], this effect can be explained in terms of electronic band structure. The gain in the kinetic energy of the valence electrons, due to band splitting, is partially counter-balanced by an increase in the volume. Since the magnetic moments are determined by band splitting, the ω_s values will be proportional to the volume. It is thus expected that the magneto-volume coupling scales linearly with the difference between the squares of the magnetic moments. The above prediction is fulfilled in γ- Fe_xM_{100-x} alloys with M=Pd or Pt –Fig.10b.

3.2 Crystallographically ordered compounds

The total energies as function of lattice parameters, for $FePd_3$ and as function of volumes for FePd compound are shown in Fig.11. The stable solutions are ferromagnetic. The atom resolved spin polarized density of states (DOS), determined, at equilibrium lattice constants, are given in Fig.12. The majority spin sub-bands are almost filled, the states at the Fermi level having mainly spin minority character. As in solid solutions, due to Fe3d-Pd4d exchange interactions, the Pd4d band is split. The induced Pd4d band polarization is higher in FePd than in $FePd_3$ and can be correlated with a smaller number of iron atoms involved in short range exchange interactions, in $FePd_3$, as compared to FePd. The Pd4d band polarizations are paralelly oriented to iron moments. The computed magnetic moments per formula unit agree rather well with experimental values-Table1.

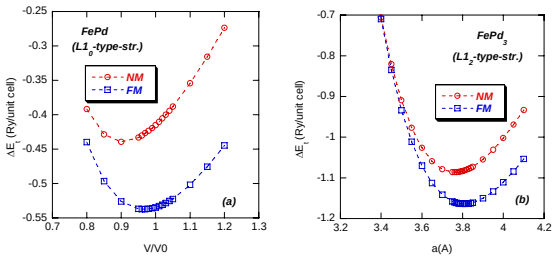

Fig. 11.Total energies of ferromagnetic and non-magnetic states in $FePd_3$ and FePd compounds.

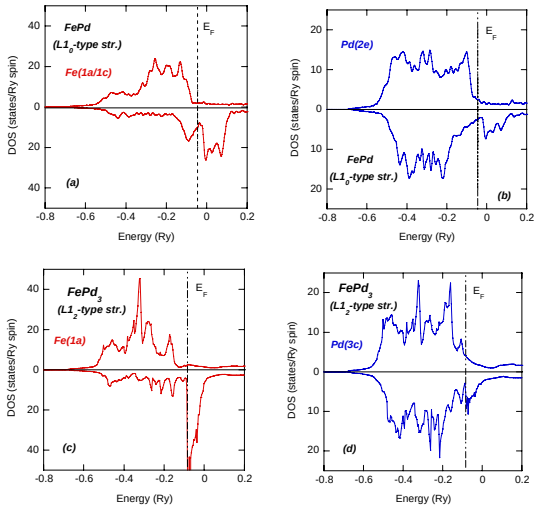

Fig. 12. Density of states for Fe and Pd atoms in FePd (a,b) and $FePd_3$ (c,d) compounds.

Table 1. Computed lattice constants, magnetic moments and the corresponding experimental values for Fe-Pd alloys.

Compound	Crystal structure	Lattice constants (Å)		Atom	l	m_l (μ_B)	m_{total}(calc./exp.) (μ_B/atom)	M (μ_B/f.u.)	
		calc.	exp.					calc.	exp.
α-$Fe_{95}Pd_5$	$Im\bar{3}m$ (bcc)	2.81	2.90 [16]	Fe(2a)	0	-0.004	2.271 (calc.)	2.178	2.20 [16] (5.4 at % Pd)
					1	-0.044			
					2	2.319			
				Pd(2a)	0	-0.014	0.417 (calc.)		
					1	-0.055			
					2	0.486			
α-$Fe_{90}Pd_{10}$	$Im\bar{3}m$ (bcc)	2.84	2.92 [16]	Fe(2a)	0	-0.004	2.428 (calc.)	2.228	2.26 [16] (9 at % Pd)
					1	-0.041			
					2	2.473			
				Pd(2e)	0	-0.016	0.424 (calc.)		2.39 [3] (9.4 at % Pd)
					1	-0.052			
					1	0.492			
α-$Fe_{85}Pt_{15}$	$Im\bar{3}m$ (bcc)	2.87	2.93 [16]	Fe(2a)	0	-0.003	2.550 (calc.)	2.230	2.25 [16]
					1	-0.039			
					2	2.592			
				Pd(2a)	0	-0.016	0.420 (calc.)		
					1	-0.051			
					2	0.487			
γ-Fe_{75} Pd_{25}	$Fm\bar{3}m$ (fcc)	3.67	3.68 [49]	Fe(4a)	0	-0.008	2.615 (calc.)	2.046	
					1	-0.043			
					2	2.666			
				Pd(4a)	0	-0.023	0.337 (calc.)		
					1	-0.055			
					2	0.415			
γ-Fe_{50} Pd_{50}	$Fm\bar{3}m$ (fcc)	3.77	3.75 [49]	Fe(4a)	0	-0.001	2.823 (cal.)	1.577	1.604 [20]
					1	-0.028			
					2	2.852	2.85 (exp.) [20]		1.586 [10]
				Pd(4a)	0	-0.018	0.331 (calc.)		
					1	-0.043			
					2	0.392	0.358 (exp.) [20]		
γ-Fe_{25} Pd_{50}	$Fm\bar{3}m$ (fcc)	3.75	3.86 [49]	Fe(4a)	0	-0.013	3.025 (calc.)	1.041	1.004 [20]
					1	-0.004			
					2	3.042	2.98 (exp.)[20]		
				Pd(4a)	0	-0.010	0.340 (calc.)		
					1	-0.024			
					2	0.374	0.345 (exp.) [20]		
FePd	P4/mmm ($AuCu$-$L1_0$)	a=3.801 c=3.664	a=3.855 c=3.714 [49]	Fe(1a/1c)	0	-0.006	2.808 (calc.) 3.010 (exp.) [19]	6.418	6.620 [19]
					1	-0.020			
					2	2.834			
				Pd(2e)	0	-0.019	0.401 (calc.) 0.300 (exp.) [19]		
					1	-0.059			
					2	0.479			
$FePd_3$	$Pm\bar{3}m$ ($AuCu_3$-$L1_2$)	3.81	3.85 [49]	Fe(3c)	0	0.007	3.177 (calc.) 3.100 (exp.) [20] 2.700 (exp.) [21]	3.990	4.360 [20] 4.410 [21]
					1	0.024			
					2	3.146			
				Pd(1a)	0	-0.014	0.271 (calc.) 0.420 (exp.) [20] 0.570 (exp.) [21]		
					1	-0.040			
					2	0.325			

The FePd compound shows a tetragonal structure, where two types of iron atoms are present. For equilibrium lattice constants the Fe1a sites have 4Fe1c atoms situated at 2.69 Å, 2Fe1a ones at 3.66 Å and 4Fe1a atoms situated at 3.80 Å and Fe1c has 4Fe1a at 2.69 Å, 2Fe1c at 3.66 Å and 4Fe1c at 3.80 Å.

The variation of the iron moments and Pd4d band polarizations in FePd and $FePd_3$ as function of volumes and lattice parameters, respectively, are shown in Fig.13. No evidence for a "non-magnetic" state is shown at $v/v_0 \geq 0.8$ (FePd) or $a/a_e \geq 0.8$ ($FePd_3$). The smallest distance between iron atoms in FePd, if the compound is uniformly compressed, involves s values close to those corresponding to s=1.06 Å, for $v/v_0 \cong 0.8$. In this compound, there are two types of iron atoms situated at different distances, the exchange interactions being more complex than in cubic structure. By reducing volume, as effect of pressure, the Fe1a-Fe1c exchange interactions can be negative. The exchange interactions between Fe1a-Fe1a, remain positive, since even at the reduction of volume at 80 %, values s > 1.06 Å are shown. Since of higher number of neighbouring iron atoms occupying the Fe1a type of sites, the positive

exchange interactions are strongest than the negative ones and consequently the last ones can not be satisfied.

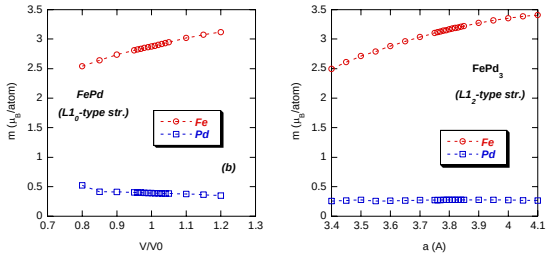

Fig. 13. The dependence of the iron and palladium moments as function of volume in FePd and of lattice parameters in $FePd_3$ compounds.

In case of $FePd_3$ compound, for equilibrium lattice constant, the Fe1a atoms has 12 Pd3c situated at 2.694 Å and 6Fe1a at 3.81 Å. Since of disordering effects and/or variation from stoichiometric composition, the Fe atoms can occupy also Pd sites. In both cases the s values are higher than 1.06 Å, suggesting the presence of ferromagnetic type behaviour. As the lattice constant is reduced to 80 %, the Fe1a-Fe1a distances are higher than that corresponding to s= 1.06 Å. Some antiferromagnetic interactions can appear only if Fe enters also in Pd sites, since $d_{Fe\text{-}Pd}$ is smaller than 2.5 Å.

The effect of pressure on the magnetic behaviour of Pd_3Fe was studied [62]. Zero temperature DFT calculations, identified a ferromagnetic ground state and showed also several antiferromagnetic states, with comparable energies, at p>20 GPa. A collapse of the iron magnetic moment was shown at 300 K in the pressure range $8.9 \leq p \leq 12.3$ GPa. This can be correlated with the diminution of Curie temperature, the variation of magnetization as function of T/T_c, respectively. It is thus possible that the Curie temperatures, at the above pressures, to decrease below RT, in agreement with Néel-Slater curve.

4. Conclusions

The total energy calculations on γ-Fe_xPd_{100-x} and α-Fe_xPd_{100-x} solid solutions were performed. The determined equilibrium lattice constants describe well the experimental values. The composition dependences of the iron magnetic moments and Pd4d band polarizations have been obtained. Both in γ- and α- solid solutions there is an increase of Pd band polarization in a limited composition range, as the Fe content increases, and then saturates. The iron moments increase as function of Pd content. The observed behaviour was correlated with short range Fe3d-Pd4d exchange interactions, hybridization effects, respectively. The computed magnetic moments per formula unit agree with experimental values. The exchange interactions and Curie temperatures were determined and compared with those experimentally obtained. The data were analysed according with Néel- Slater curve, which predict their evolution as function of the distances between iron atoms. The volume magnetostrictions were determined. These scales linearly as function of the differences between the square of magnetization in ferromagnetic and paramagnetic states.

The magnetic properties of ordered FePd and $FePd_3$ compounds were also studied and correlated with those experimentally observed.

Acknowledgements

Realized under contract 12-070/2007 with the acronym APLIMAG.

References

[1] T. B. Massalsky, Binary Alloys Phase Diagrams, ASM International Materials Park, Ohio, 1986
[2] H. Yabe, T. Kuji, J. Metastable Nanocryst. Mater. **24-25**, 439 (2005)
[3] H.Yabe, R.C. O'Handley, T. Kuji, J. Magn. Magn. Mat. **310**, 2500 (2007)
[4] M. Sugiyama, R. Oshima, F. E. Fujita, Trans. Jpn. Inst. Met. **25**, 585 (1984)
[5] E. C. Bain, Trans Am. Inst. Min. Met. Eng. **70**, 25 (1924)
[6] L. Wang, Z. Fan, A.G. Roy and D.E. Laughlin, J. Appl. Phys. **95**, 7483 (2004)
[7] A. Kussmann and K. Jessen, J. Phys. Soc. Jpn. **17**, 136 (1962)
[8] E. F. Wassermann, Physica Scripta **T25**, 209 (1989), J. Magn. Magn. Mat. **100**, 346 (1991)
[9] J. Koeda, Y. Nakamura, T. Fukada, T. Kakeshita, T. Takeuchi, K. Kishio, Trans. Mat. Res. Soc. Jpn. **26**, 215 (2001)
[10] M. Matsui and K. Adachi, Physica B **161**, 53 (1989)
[11] M. Matsui, K. Adachi, J. Magn. Magn. Mat. **31-34**, 115 (1983)
[12] M. Fallot, Ann. Phys. (Paris) **10**, 291 (1938)
[13] A.M. Clogston, B.T. Matthias, M. Peter, H.J. Williams, E. Corenzwit and R.C. Sherwood, Phys. Rev. **125**, 541 (1962)
[14] M.F. Collins and G.C.Low, Proc. Phys. Soc. London, **86**, 535 (1965)
[15] G.J. Nieuwenhuys, Adv. Phys. **24**, 515 (1975)
[16] M. Birsan, B. Fulz and L. Anthony , Phys. Rev. **B 55**, 11502 (1997)
[17] V.V. Kuprina, A. T. Grigoriev, Russ. J. Inorg. Chem. **4**, 297 (1959)
[18] G. Longworth, Phys. Rev. **172**, 572 (1968)
[19] J. Lyubina, O.Gutfleish and O. Isnard, J.Appl. Phys. **105**, 07A717 (2009)
[20] D. Adachi, D. Bonnenberg, J. J. M. Franse, R. Gersdorf, K.A. Hempel, K. Kanematsu, S. Misawa, M. Shiga, M.B. Stearns and H.P.J. Wijn, Landolt Börnstein Handbuch, vol. 19a, Springer Verlag, 1992.
[21] A. J. Smith, W. G. Sterling, T. M.Holden, J. Phys. **7**, 2411 (1977)

[22] N. N. Delyagin, A. L. Erzinkyan, V. P. Parfenova and S. I. Reyman, J. Exp. Theor. Phys. **95**, 1056 (2002)
[23] Y. Tsunoda, R. Abe, Physica B, **237-238**, 458 (1997).
[24] L. Cheng, Z. Altounian, D.H. Ryan, J.O. Ström-Olsen, M. Sutton, Z. Tun, Phys. Rev. B **69**, 144403 (2004)
[25] I. Galanakis, S. Ostanin, M. Alouani, H. Dreyssé and J.M. Wills, Phys. Rev. B **61**, 599 (2000)
[26] P. Ravindran, A.Kjekshus, H. Fjellvåg, P. James, L. Nordstrom, B. Johansson and O. Eriksson, Phys. Rev. B **63**, 144409 (2001)
[27] D. Garcia, R. Casero, M. Vázquez and A. Hernando, Phys. Rev. B **63**, 104421 (2004)
[28] H. Yamada, H. Shimizu, K. Yamamoto, K. Uebayshi, J. Alloys Compd. **415**, 31 (2006)
[29] K. Uebayashi and H. Yamada, J. Magn. Magn. Mat. **310**, 1051 (2007)
[30] P. Mohn, E. Supanetz and K. Schwarz, Aust. J. Phys. **46**, 651 (1993)
[31] T. Mohri, Y. Chen, J. Alloys Compd. **383**, 23 (2004)
[32] A.M. Mazzone, Model. Simul. Mater. Sci. Eng. **8**, 13 (2000).
[33] E.A. Gonzalez, P.V. Jasen, N.J. Castellani and A. Juan, J. Phys. Chem. Solids **65**, 1799 (2004)
[34] A. Sakuma, S. Yuasa, H. Miyajima and Y. Otani, J. Phys. Soc. Jpn. **64**, 4914 (1995)
[35] S.V. Barabash, R.Y. Chepulskii, V. Blum and A. Zunger, Phys. Rev. B **80**, 220201(2005)
[36] R.A. Stern, S.D. Willoughby, A. Ramirez, J.M. MacLaren, J. Cui, Q. Pan and R.D. James, J. Appl. Phys. **91**, 7818 (2002)
[37] J. Buschbeck, I. Opahle, S. Fähler, L. Schultz, M. Richter, Phys. Rev. B **77**, 174421 (2008)
[38] J.P. Perdew and Y. Wang, Phys. Rev. B **45**, 13244 (1992)
[39] R.R. Duplessis, R.A. Stern and J. MacLaren, J. Appl. Phys. **95**, 6589 (2004)
[40] B. Drittler, N. Stefanou, S.Blügel, R. Zeller and P.H. Dederichs, Phys. Rev. B **40**, 8203 (1989)
[41] I. Opahle, K. Koepernik, U. Nitzsche and M. Richter, Appl. Phys. Lett. **94**, 072508 (2009)
[42] S. Yuasa, H. Miyajima, Y. Otani and A. Sakuma, J.Phys. Soc. Jpn. **64**, 4906 (1995)
[43] C.A. Kuhnen, E.Z. da Silva, Phys. Rev. B **46**, 8915 (1992).
[44] P. Vlaic and E. Burzo, J. Optoelectron. Adv. Mater. **12**, 1114 (2010); AIP Conf. Proc. **1203**, 3241 (2009)
[45] O. K. Anderson and O. Jepsen, Phys. Rev. Letters **53**, 2571 (1984).
[46] I. Turek, V. Drchal, J. Kudrnovský, M. Šob, P. Weinberger, Electronic Structures of Disordered Alloys, Surfaces and Interfaces, Kluwer Academic, Boston, 1997
[47] S.H. Vosko, L. Wilk, M. Nusair, Can. J. Phys. **58**, 1200 (1980)
[48] A.J. Pindor, J.B. Stauton, G.M. Stocks, H. Winter, J.Phys. F: Metal Phys. **13**, 979 (1983)
[49] P. Villars, L.D. Calvert, Pearsosn's Handbook of Crystallographic Data for Intermetallic Phases, 2nd ed., ASM International, Materials Park, OH, 1991
[50] L. Chioncel, E. Burzo, J. Optoelectron. Adv. Mater. **8**, 1105 (2006)
[51] J. Vogel, A. Fontaine, V. Cros, F. Petroff, J. P. Kappler, G. Krill, A. Rogalev, J. Goulon, Phys. Rev.B **55**, 3663 (1997)
[52] L.Néel, Ann. Phys. Phys. (Paris) **8**, 237 (1937)
[53] F. Ono, H. Kanematsu, N.Q. Sun, Y. Matsushim, M. Matsushita, Proc. Joint. 20th AIRAPT-43th EHPRG Conferences, Kalrsruhe, Germany, 2005
[54] M. Matsushita, T. Nishimura, S. Endo, M. Ishizuka, K. Kindo, F. Ono, J. Phys.: Cond. Matter **14**, 10753 (2002)
[55] D. Givord, R. Lemaire, IEEE Trans. Magn. MAG-**10**, 109 (1974)
[56] E. Burzo, Rep. Progr. Phys .**61**, 1099 (1998); E. Burzo, W. Kappel, M. Codescu, E. Helerea, J. Optoelectron. Adv. Mater **11**, 229 (2009); E. Burzo, A.T. Pedziwiatr, W.E. Wallace, Solid State Commun, **61**, 57 (1987)
[57] E. Burzo, L.Stanciu, W.E.Wallace, J. Less Common Met. **111**, 83 (1985): A.T.Pedziwiatr, W.E. Wallace, E. Burzo and V. Pop, Solid State Commun. **61**, 61 (1987); E. Burzo, V. Pop, N. Plugaru, L. Stanciu , W.E. Wallace, Solid State Commun. **58**, 803 (1986)
[58] M. Valeanu, N. Plugaru and E. Burzo, Solid State Commun. **89**, 519 (1994)
[59] B. Khmelevskyi, A.V. Ruban, Y. Kakehashi, P. Mohn B. Johansson, Phys. Rev. B **72**, 064510 (2005)
[60] S. Khmelevskyi, I. Turek, P. Mohn, Phys. Rev. Lett. **91**, 037201 (2003)
[61] R. Hayn and V. Drchal, Phys. Rev. B **58**, 4341 (1998)
[62] M.L. Winterrose, M. S. Lucas, A. F. Yue, I. Halevy, L. Mauger, J. A. Muñoz, J.Z. Hu, M. Lerche, B. Fultz, Phys. Rev. Lett. **102**, 237202 (2009).

*Corresponding author: emil.burzo@phys.ubbcluj.ro